COMPRESSIBILITY EFFECTS ON SHOCK-TURBULENCE INTERACTION

Stéphane Jamme[1], Florence Torres[1], Jean-Bernard Cazalbou[1] and Patrick Chassaing[1][2]

[1] Département de Mécanique des Fluides, E.N.S.I.C.A.
1 Place Emile Blouin, 31056 Toulouse Cedex, France

[2] Institut de Mécanique des Fluides de Toulouse
Allée du Professeur Camille Soula, 31400 Toulouse, France

ABSTRACT

Direct Numerical Simulation (DNS) and inviscid linear analysis (LIA) are used to study the interaction of a normal Mach 1.5 shock wave and isotropic turbulence. The influence of the nature of the incoming turbulence on the interaction is emphasized. The presence of upstream entropy fluctuations enhance the amplification of the turbulent kinetic energy and transverse vorticity variance across the shock compared to the solenoidal (pure vorticity) case. More reduction of the transverse Taylor microscale is also observed in the vorticity-entropy case while no influence can be seen on the longitudinal microscale. When acoustic and vortical fluctuations are associated upstream, less amplification of the kinetic energy, less reduction of the transverse microscale and more amplification of the transverse vorticity variance are observed through the discontinuity. Most of these effects have been reported previously by different authors using different numerical codes. In our case, all calculations are conducted with the same numerical tool and similar flow parameters, so that the observed influence of upstream turbulence cannot be attributed to differences in the numerics. All the DNS results are in good qualitative agreement with LIA.

INTRODUCTION

The interaction of turbulent boundary layers or turbulent supersonic jets with a shock wave is certainly one of the most important topic for transonic and supersonic aeronautics. However, the complex nature of these flows prevents to achieve a detailed understanding of the basic mechanisms involved in shock-turbulence interaction since additional phenomena such as flow separation or wall proximity effects are usually present. A more basic approach of the problem that allows to isolate the physics of the process is to consider the interaction between isotropic turbulence and a normal shock wave.

Numerous studies have been conducted in this field. The first ones were theoretical works that relied on linear analysis and Kovasznay's modal decomposition of turbulence (Kovasznay, 1953). They developed the so-called Linear Interaction Analysis (LIA) (Ribner, 1953 - Moore, 1953) which was recently revisited and completed by Lee et al. (1993) and Mahesh et al. (1995, 1997). Experimental research has also been conducted using shock tubes and wind tunnels (see e.g. Barre et al., 1996 for a review). Since the early 1990's, numerical simulations of shock-turbulence interaction began to emerge (Rotman, 1991 - Lee et al., 1993, 1997 - Hannappel and Friedrich, 1995 - Mahesh et al., 1997). All the works cited above agree in predicting the evolutions of some characteristics of turbulence across the shock wave such as the amplification of the turbulent kinetic energy and vorticity variances. Many aspects of the problem are now quite well understood even if contradictions still exist concerning other features of the flow like for instance the behaviour of turbulent length scales across the discontinuity. Moreover, most of these works investigated the interaction between shock waves and solenoidal turbulence, except in the latest studies. Mahesh et al. (1995, 1997) used both DNS and LIA to show that upstream entropy fluctuations may strongly modify the behaviour of a turbulent flow across the shock. Similarly, Hannappel and Friedrich (1995) reported that compressible upstream turbulence behaves differently during the interaction than incompressible turbulence.

The purpose of this work is to address this question by comparing the evolution across a same shock wave of

three different turbulent flows generated using Kovasznay's modal decomposition of turbulence. The simulations were conducted with the same numerical tool and the same flow parameters in order to be sure that the differences between the three cases are only due to the nature of the upstream turbulence. We also reproduced the latest developments of LIA for the three modes of turbulence (Jamme, 1998) in order to compare with our DNS results. In the following sections, the numerical procedure is first presented before giving the main results of the simulations.

THE NUMERICAL APPROACH

Description of the method

We developed a numerical tool allowing the resolution of the 3D time-dependent Navier-Stokes equations without any modelling. The non-dimensional equations of mass, momentum and energy are considered along with the equation of state for a perfect gas. A constant volume specific heat ratio of $\gamma = 1.4$ is assumed and Sutherland's law is used to relate viscosity to temperature. The equations are written in conservative form and the numerical scheme is a finite volume version of the explicit predictor/corrector MacCormack scheme which is second order accurate in space and time (MacCormack, 1969).

All the simulations presented in this paper were conducted on the IBM RISC System/6000 SP2 of the laboratory. We used a parallel version of the code based on a domain decomposition approach.

Test cases

In order to assess the ability of the code to resolve our problem, we considered various test cases before the main configuration. In a first step, we evaluated the behaviour of our numerical tool regarding the two components of the interaction considered separately. First, we tested the ability of the code to resolve laminar weak shock waves, then we concentrated on temporal and spatial simulations of decaying isotropic turbulence. We won't give any details on the above test cases and we only mention that they demonstrated a good behaviour of the MacCormack scheme provided the shock Mach number M_1 and the turbulent Reynolds number Re_λ of the upstream flow are sufficiently low for a given dicretization grid.

A more interesting situation is to consider the two-dimensional interaction between a shock and a plane vorticity-entropy wave since it allows a direct comparison with LIA results. This is what is described below.

We present numerical results of the interaction of a sinusoidal vorticity-entropy wave with a Mach 1.5 shock wave. The parameters of the computations are identical to those used in the DNS presented in the next sections ($Re_r = 13.4$, $M_r = 0.1$, $Pr = 0.7$). The computational

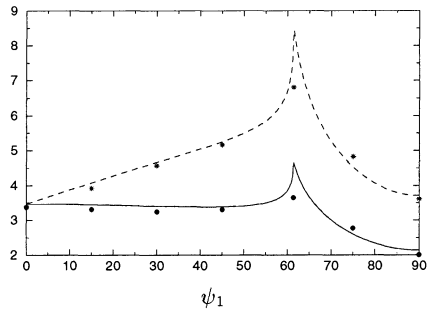

Figure 1: Amplification of vorticity ($\overline{\omega_2'^2}/\overline{\omega_1'^2}$) across the shock as a function of the angle of incidence - $M_1 = 1.5$. Comparison DNS/LIA : (——) LIA [$A_e = 0$, $A_v = 2.5\%$]; (•) DNS [$A_e = 0$, $A_v = 2.5\%$]; (– – –) LIA [$A_e = A_v = 2.5\%$]; (∗) DNS [$A_e = A_v = 2.5\%$].

domain has dimensions of 2π in both directions. A non-uniform grid that clusters points near the discontinuity is used in the streamwise direction x_1. In the present case, about 15 mesh points are located inside the shock wave. A uniform mesh of 32 points is used in the transverse direction x_2. The flow is initialized by a steady normal shock wave (obtained with a preliminary calculation) over which the fluctuating vorticity-entropy wave is superposed at $t = 0$:

$$\begin{cases} u_1' = U_1 A_v \sin\psi_1 \cos(k_x x + k_y y) \\ v_1' = -U_1 A_v \cos\psi_1 \cos(k_x x + k_y y) \\ \rho_1' = \overline{\rho}_1 A_e \cos(k_x x + k_y y) \\ p_1' = 0 \end{cases} \tag{1}$$

where the subscript '1' refers to upstream values and the overbars denote mean quantities. The wavenumbers k_x and k_y are given by :

$$k_x = k\cos\psi_1 \qquad k_y = k\sin\psi_1 \tag{2}$$

where k is the magnitude of the wavenumber vector and ψ_1 denotes the angle between the wavenumber vector and x_1. The variables A_v and A_e correspond to the intensity of velocity and density upstream of the shock wave. They were both equal to 0.025. Periodic boundary conditions are specified in the transverse direction whereas approximately non-reflecting boundary conditions (Thompson, 1987, 1990) are used at the outflow boundary in the streamwise direction. At the inflow boundary ($x_1 = 0$), we superpose to the mean flow values ($\overline{u}_1 = U_1$, $\overline{u}_2 = 0$, $\overline{p} = \dfrac{1}{\gamma M_r^2}$, $\overline{\rho} = 1$) an unsteady wave that takes the following form :

$$\begin{cases} u_1' = U_1 A_v \sin\psi_1 \cos(k_y y - U_1 k_x t) \\ v_1' = -U_1 A_v \cos\psi_1 \cos(k_y y - U_1 k_x t) \\ \rho_1' = \overline{\rho}_1 A_e \cos(k_y y - U_1 k_x t) \\ p_1' = 0 \end{cases} \tag{3}$$

Several incidence angles (ψ_1) were considered inside the interval $[0; \pi/2]$. For each case, the wavenumber k

was choosen so that we have one wavelength in the x_2 direction :

$$k_y = k \sin \psi_1 = 1 \qquad k_x = 1/\tan \psi_1 \qquad (4)$$

The statistics of the flow were gathered after one flow-through time in order to let the initial transient exit the domain and covered one period of the incident disturbance.

The behaviour of the code during the interaction is evaluated by comparing the values obtained for the amplification of vorticity fluctuations ($\overline{\omega_2'^2}/\overline{\omega_1'^2}$) to the linear analysis predictions. The results are plotted in figure 1 for the two cases we considered : the first one corresponds to a solenoidal incident wave ($A_e = 0$, $A_v = 2.5\%$) and the second one concerns a vorticity-entropy wave ($A_e = A_v = 2.5\%$). Excellent agreement between computation and analysis is seen away from the critical angle $\psi_c = 61.36°$: the difference between the two approaches never exceeds 5%. When ψ_1 goes to ψ_c, Mahesh et al. (1996) showed that LIA may be questionable : the deviation around the critical angle is thus a limitation of the linear analysis, not of the computation.

All the tests we conducted lead us to conclude that reliable DNS of shock-turbulence interaction was possible using our numerical tool, even if there are obvious limitations in terms of resolution and Mach numbers using this kind of code.

Main computations

Flow configuration. The shock-turbulence interaction problems presented hereafter are studied in the cubic domain of $(2\pi)^3$ sketched in figure 2. Periodic boundary conditions are specified in the two transverse directions of the flow (x_2 and x_3), but not in the direction normal to the shock which is not homogeneous. In this direction, statistically steady turbulent data are prescribed as inflow conditions and all variables are specified since the flow is supersonic. These turbulent conditions come from several developed fields obtained with the preliminary simulations (see next section). They are added to the mean advection variables of the flow ($\overline{u}_1 = U_1$, $\overline{u}_2 = \overline{u}_3 = 0$, $\overline{p} = \frac{1}{\gamma M_r^2}$, $\overline{\rho} = 1$) in the inflow plane and updated at each time step. The outflow is subsonic and the first-order characteristic boundary conditions of Thompson (1987, 1990) are used. These conditions give the outflow plane a non-reflective character which is not physically correct but allows to minimize the influence of an unknown outside in the computational approximation.

At the initial time of the calculation, a laminar plane shock wave at Mach 1.5 is created using the Rankine-Hugoniot relations. It is maintained in the middle of the computational box so that the mean flow is steady (its mean position remains fixed and the computational

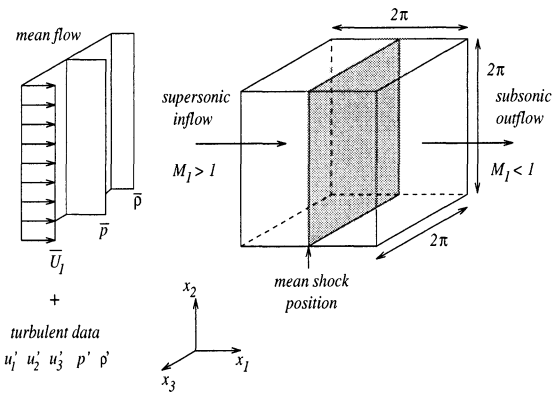

Figure 2: Sketch of the computational domain.

domain moves at the shock speed). In order to save time in the setting-up of the shock, a pre-calculation is conducted for the shock alone, until its initial profile becomes a stable solution of the Navier-Stokes equations. In order to allow the resolution of the shock without oscillations, we use a stetched grid in the streamwise direction with clustered points near the discontinuity. A regular grid is used in the transverse directions.

Inflow conditions. The turbulent data we superpose to the mean flow at the entrance of the computational domain come from several developed turbulent fields created independently. These fields are obtained with preliminary simulations of temporally decaying isotropic turbulence. Three types of turbulences were considered. The first one is solenoidal, the second one contains vorticity and entropy fluctuations (which satisfy Morkovin's hypothesis : $\frac{\rho_{rms}}{\overline{\rho}} = \frac{T_{rms}}{\overline{T}} = (\gamma - 1) M_1^2 \frac{u_{1\,rms}}{U_1}$), and the third one contains vorticity and pressure fluctuations. The procedure we used to obtain these data in the two last cases is similar to that of Mahesh et al. (1997) or Hannappel and Friedrich (1995).

RESULTS AND DISCUSSION

Parameters of the simulations

We present in this section some results obtained with the following non-dimensional parameters : $Re_r = \frac{\rho_r^* u_r^* L_r^*}{\mu_r^*} = 13.4$; $M_r = \frac{u_r^*}{c_r^*} = 0.1$ and $Pr = 0.7$; where f_r^* refers to a dimensional reference variable. The turbulence characteristics in the inflow plane of the numerical box are the following : $Re_\lambda = Re_r \frac{\lambda u_{1\,rms}}{\overline{\nu}} = 6.7$; $M_t = \frac{q}{\overline{c}} = \frac{\sqrt{\overline{u_i' u_i'}}}{\overline{c}} = 0.173$; $u_0 = 1$ and $k_0 = 4$ (where $u_0 = u_{1\,rms} = u_{2\,rms} = u_{3\,rms}$ and k_0 refers to the

	I1.5sol	I1.5ent	I1.5ac
$Re_\lambda = Re_r \frac{u_{1_{rms}}\lambda}{\overline{\nu}}$	6.7	6.7	5
$M_t = \frac{\sqrt{q^2}}{\overline{c}}$	0.173	0.173	0.173
$q^2/2$	1.5	1.5	1.5
$S = \sum_{\alpha=1}^{3} \frac{\overline{(u'_{\alpha,\alpha})^3}}{\overline{(u'_{\alpha,\alpha})^2}^{3/2}}$	-0.45	-0.43	-0.46
$u_{1_{rms}}/U_1$	0.067	0.067	0.067
$p_{rms}/\overline{p}$	0.021	0.026	0.146
$\rho_{rms}/\overline{\rho}$	0.017	0.058	0.103
$T_{rms}/\overline{T}$	0.006	0.056	0.042
$(\gamma-1)M_1^2 u_{1_{rms}}/U_1$	0.06	0.06	0.06
$\overline{u_1'T'}/u_{1_{rms}}T_{rms}$	0.008	-0.91	-0.02

Table 1: Turbulence features in the inflow plane.

most energetic wavenumber of the turbulent flow). The shock Mach number is $M_1 = 1.5$, and the grid entails 210×128^2 points. Three different simulations were conducted with the above parameters. The only difference between them lies in the nature of the upstream turbulent flow. The following convention is adopted hereafter : I1.5sol refers to the solenoidal case, I1.5ent to the vorticity/entropy case and I1.5ac to the vorticity/pressure case. Table 1 summarizes the features of the three different incident flows in the inflow plane.

Statistics of the flow are gathered when a statistically steady state is established in the computational domain (typically after one flow-through time) so that averaging may be performed in time. The ensemble Reynolds average is then approximated by taking spatial averages in the two homogeneous directions and additional time averages performed over 60 fields saved during the simulation. The ensemble average of a variable f and its deviation from the mean will be respectively noted $\overline{f}$ and f'. We also introduce the Favre's mass-weighted average $\tilde{f} = \frac{\overline{\rho f}}{\overline{\rho}}$, with : $f = \tilde{f} + f''$.

Details of the comparisons

Turbulent velocity fluctuations. We present in figures 3(a) and 3(b) the spatial evolutions of the normal Reynolds stresses $\widetilde{u_1''^2}$ and $\widetilde{u_2''^2}$ in the three simulations. The non-monotonic behaviour of $\widetilde{u_1''^2}$ immediately behind the shock is a known feature of isotropic turbulence-shock wave interaction (see Lee et al., 1993 - Hannappel and Friedrich, 1995 - Mahesh et al, 1997

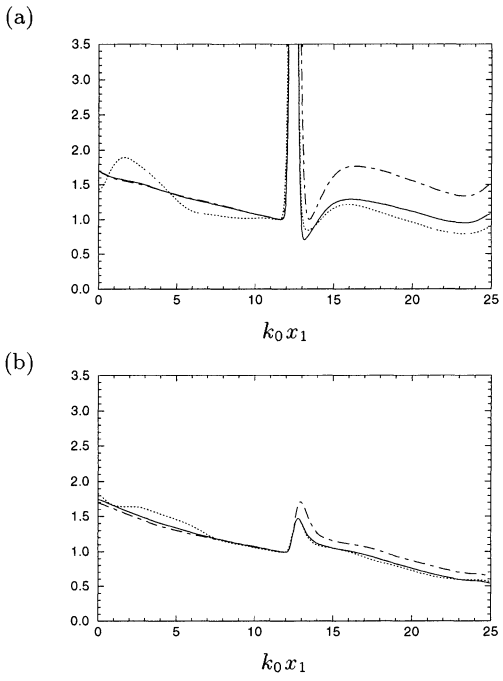

Figure 3: Spatial evolutions of $\widetilde{u_1''^2}$ (a) and $\widetilde{u_2''^2}$ (b) normalized by their value immediately upstream of the shock - DNS. (——) I1.5sol, (– · –) I1.5ent, (· · · · ·) I1.5ac.

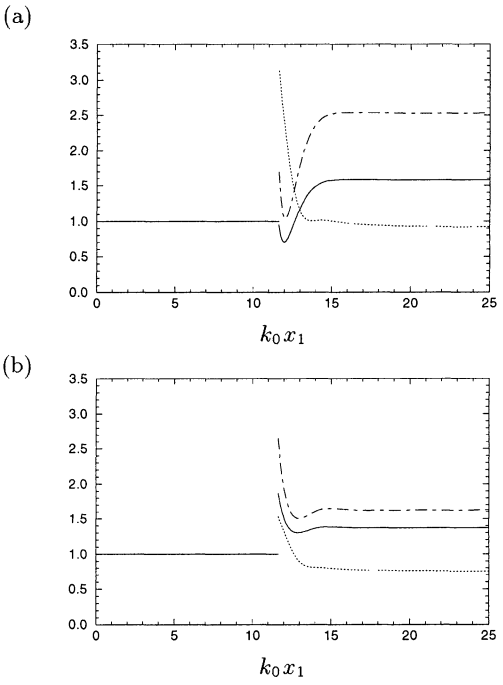

Figure 4: Spatial evolutions of $\widetilde{u_1''^2}$ (a) and $\widetilde{u_2''^2}$ (b) normalized by their value upstream of the shock - LIA. (——) pure vorticity case, (– · –) vorticity/entropy case, (· · · · ·) pure acoustic case.

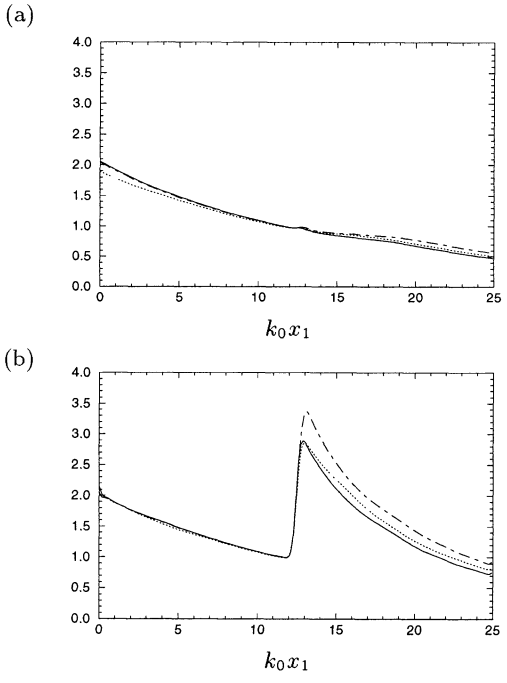

Figure 5: Spatial evolutions of $\overline{\omega_1'^2}$ (a) and $\overline{\omega_2'^2}$ (b) normalized by their value immediately upstream of the shock. (——) I1.5sol, (— · —) I1.5ent, (· · · · ·) I1.5ac.

- Jamme, 1998). Investigation of the budgets for these quantities (not shown here) indicates that the pressure-work term $\left(-\overline{u_i'' \frac{\partial p'}{\partial x_i}}\right)$ is responsible for this behaviour.

We can notice a clear influence of the nature of the incident flow on the interaction. The presence of upstream entropy fluctuations satisfying Morkovin's hypothesis increases the level reached by the Reynolds stresses far behind the shock wave (mainly for the streamwise component). On the other hand, the presence of non-negligible pressure fluctuations in the incoming turbulence seems to slightly reduce the far field level of $\widetilde{u_1''^2}$ and $\widetilde{u_2''^2}$. These observations are in good qualitative agreement with LIA (see figure 4), but a quantitative comparison between DNS and LIA is much more difficult since the conditions are not exactly the same in both approaches : when entropy fluctuations are present, Morkovin's hypothesis holds exactly in the analysis whereas it is approximatly satisfied in DNS. On the other hand, the I1.5ac simulation corresponds to an incident flow containing pressure and vorticity fluctuations whereas the corresponding case in the analysis deals with a pure acoustic turbulent flow upstream of the shock. Moreover, LIA refers to an inviscid approach of the problem. In the simulations, the very low turbulent Reynolds number ($Re_\lambda = 6.7$) is responsible for non-negligible viscous effects.

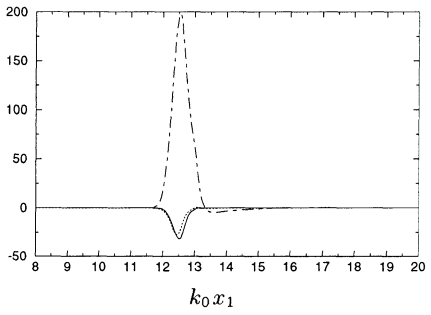

Figure 6: Comparison of the baroclinic torque calculated in the budgets of $\overline{\omega_2'^2}$. (——) I1.5sol, (— · —) I1.5ent, (· · · · ·) I1.5ac.

Vorticity variances. The same kind of comparisons for the vorticity variances are made in this section.

No major difference between the three cases appears for the streamwise component $\overline{\omega_1'^2}$, whereas the amplification of $\overline{\omega_2'^2}$ is seen to increase by 19.3% in the case I1.5ent compared to I1.5sol (see figure 5). This is once again in good qualitative agreement with LIA which predicts no amplification of $\overline{\omega_1'^2}$ in any case and an increase of 31.5% in the amplification factor of $\overline{\omega_2'^2}$ when upstream entropy fluctuations are present (the solenoidal case is still the reference). Mahesh et al. (1997) proposed an explanation based on the relative effects of bulk compression and baroclinic torque to understand the influence of entropy fluctuations. This proposal is confirmed by our DNS results. As a matter of fact, in both cases (I1.5sol and I1.5ent), the budgets of the transverse vorticity show that bulk compression is responsible for the amplification of $\overline{\omega_2'^2}$. Moreover, the relative importance of bulk compression is the same in both cases. However, in the vorticity-entropy case, the compression by the mean flow is not the only positive contribution inside the shock and the baroclinic torque $\left(2\epsilon_{\alpha jk}\overline{\frac{1}{\rho^2}\omega_\alpha' \frac{\partial \rho}{\partial x_j}\frac{\partial p}{\partial x_k}}\right)$ also plays an important role. Figure 6 compares the importance of this term in the budgets of the transverse vorticity for the three simulations. It is clear in the I1.5ent case that the baroclinic torque is not negligible, in contradiction with what is observed in the other configurations.

When pressure fluctuations are present upstream of the shock (I1.5ac), the amplification of $\overline{\omega_2'^2}$ is also greater than in the case I1.5sol but the difference is far less important than before. This is in agreement with the DNS results of Hannappel and Friedrich (1995), even if the difference between the solenoidal and the "compressible" cases was more important in the simulations they conducted for a Mach 2 shock wave.

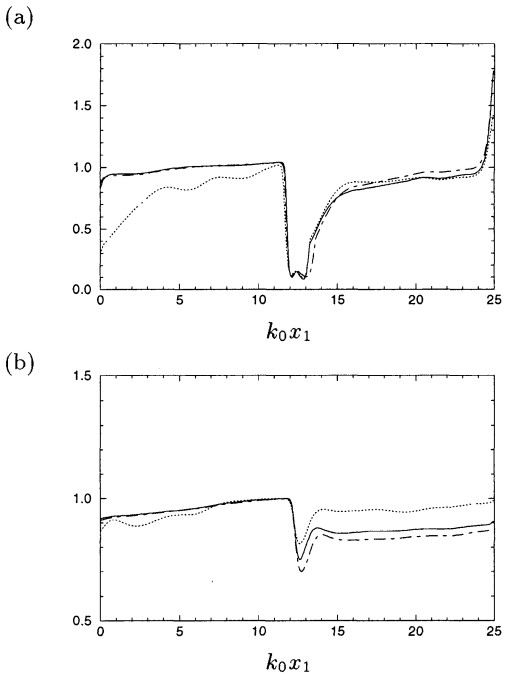

Figure 7: Spatial evolutions of λ_1 (a) and λ_2 (b) normalized by their value immediately upstream of the shock. (——) I1.5sol, (— · —) I1.5ent, (· · · · ·) I1.5ac.

Taylor microscales. We show in figures 7 the spatial evolutions of the Taylor microscales of the turbulent flows : $\lambda_\alpha = \left[\overline{u'^2_\alpha} / \overline{\left(\frac{\partial u'_\alpha}{\partial x_\alpha}\right)^2}\right]^{1/2}$.

The behaviour across the shock of these quantities is still a conflicting point in the literature between numerical and experimental works. We can only state here that our results are in agreement with all previous DNS on the topic : the Taylor microscales are reduced during the interaction (this diminution of λ_α corresponds to a gain of energy which is more pronounced in the highest part of the velocity spectra : see for instance Lee et al., 1993). If no noticeable difference appears between the three cases for λ_1, λ_2 is more reduced in the case I1.5ent : the difference amounts to 3% between I1.5sol and I1.5ent, and LIA predicts a reduction 5% more important when the upstream turbulence contains entropy fluctuations. On the other hand, λ_2 is less reduced in the case I1.5ac, which confirms Hannappel and Friedrich's conclusions.

CONCLUSION

This paper shows the sensitiveness of the shock-turbulence interaction phenomenon to the compressible nature of the upstream turbulent flow. All the preceding conclusions agree with previous recent numerical studies concerning the influence of Kovasznay's modes on the evolution of turbulence across a shock wave (Hannappel and Friedrich, 1995 - Mahesh et al., 1997). Our DNS results are also in qualitative agreement with linear analysis.

This type of fundamental study will undoubtedly be helpful to understand more complicated phenomena like the interaction between a shock and a supersonic boundary layer. In this configuration, Morkovin's hypothesis is satisfied and the presence of entropy fluctuations should strongly promote the amplification of turbulence as reported in this work.

REFERENCES

Barre S., Alem D. and Bonnet J.P., 1996, "Experimental study of a normal shock/homogeneous turbulence interaction", *AIAA J.*, Vol. 34, pp. 968-974.

Hannappel R. and Friedrich R., 1995, "Direct Numerical Simulation of a Mach 2 shock interacting with isotropic turbulence", *Applied Scientific Research*, Vol. 54, pp. 205-221.

Jamme S., 1998, "Etude de l'interaction entre une turbulence homogène isotrope et une onde de choc", PhD. Thesis, Institut National Polytechnique de Toulouse.

Kovasznay L.S.G., 1953, "Turbulence in supersonic flow", *J. of the Aero. Sci.*, Vol. 20, pp. 657-682.

Lee S., Lele S.K. and Moin P., 1993, "Direct numerical simulation of isotropic turbulence interacting with a weak shock wave", *J. Fluid Mech.*, Vol. 251, pp. 533-562.

Lee S., Lele S.K. and Moin P., 1997, "Interaction of isotropic turbulence with shock waves : effect of shock strength", *J. Fluid Mech.*, Vol. 340, pp. 225-247.

MacCormack R.W., 1969, "The effect of viscosity on hypervelocity impact cratering", AIAA Paper 69-354.

Mahesh K., Lee S., Lele S.K. and Moin P., 1995, "The interaction of an isotropic field of acoustic waves with a shock wave", *J. Fluid Mech.*, Vol. 300, pp. 383-407.

Mahesh K., Moin P. and Lele S.K., 1996, "The interaction of a shock wave with a turbulent shear flow", Report TF-69, Stanford University.

Mahesh K., Lele S.K. and Moin P., 1997, "The influence of entropy fluctuations on the interaction of turbulence with a shock wave", *J. Fluid Mech.*, Vol. 334, pp. 353-379.

Moore F.K., 1953, "Unsteady oblique interaction of a shock wave with a plane disturbance", NACA TN 2879.

Ribner H.S., 1953, "Convection of a pattern of vorticity through a shock wave", NACA TN 2864.

Rotman D., 1991, "Shock wave effects on a turbulent flow", *Phys. Fluids A*, Vol. 3, pp. 1792-1806.

Thompson K.W., 1987, "Time dependent boundary conditions for hyperbolic systems I", *J. Comp. Phys.*, Vol. 68, pp. 1-24.

Thompson K.W., 1990, "Time dependent boundary conditions for hyperbolic systems II", *J. Comp. Phys.*, Vol. 89, pp. 439-461.